



Research Article

Stage-Dependent Predation on Prey Species Who Possess Different Life Histories

Arild Wikan  and Ørjan Kristensen 

School of Business and Economics, The Arctic University of Norway-Campus, Harstad, Tromsø, Norway

Correspondence should be addressed to Ørjan Kristensen; orjan.f.kristensen@uit.no

Received 24 October 2022; Revised 5 January 2023; Accepted 9 March 2023; Published 24 March 2023

Academic Editor: Elmetwally Elabbasy

Copyright © 2023 Arild Wikan and Ørjan Kristensen. This is an open access article distributed under the Creative Commons Attribution License, which permits unrestricted use, distribution, and reproduction in any medium, provided the original work is properly cited.

Two stage-structured one-population (prey) models together with four prey-predator models are analyzed. Regarding the prey models, where one of them has fecundity elements which depend on the total population while the fecundities of the other depend on the mature part of the population only, we prove that both of them are permanent and moreover that their fixed points undergo supercritical bifurcations, flip, and Neimark-Sacker, respectively, at the various instability thresholds. By use of the models, we also provide a discussion of stability and dynamical properties of species who possess different life histories and extent results obtained elsewhere. Turning to predation, in contrast to what one finds in most papers, we scrutinize cases where both the immature subpopulation of the prey and the mature part are targets for the predator. Among our findings, here is that increased predation may act in both a stabilizing and destabilizing fashion depending on the size of fecundity of prey. Moreover, we present new results about the transition from stability to instability, and we show that whenever predation acts destabilizing, the effect is most profound in cases where the prey possesses a precocious semelparous life history. We also provide several examples where increased predation may turn a stable system chaotic.

1. Introduction

As it is well known, nonlinear discrete age- and stage-structured population models may serve as excellent tools when one wants to describe and reveal dynamical properties and behaviour of a great variety of species. The use of age-structured models, i.e., iteroparous or semelparous Leslie matrix models, rests upon the prerequisite that sexual maturity is linked to age or alternatively to other factors which are closely correlated to age. There is a vast literature of theoretical studies as well as studies applied on concrete species which make use of age-structured models. Indeed, in [1], the authors present an analysis of 2×2 Leslie matrix models where focus is on strange attractors and suggest on how elements from statistical mechanics may be applied in order to analyze chaotic behaviour. The use of Leslie matrices in order to study the dynamics of the

Oxford great tit population may be obtained in [2], and in [3], the authors apply a nonlinear iteroparous Leslie matrix model where fecundity elements do not depend on the total population but on the weighted sum of age classes in order to scrutinize the dynamical behaviour of the striped bass in the Hudson river. Referring to [4, 5], the former considers truncation effects and delay effects in large n -class models, while the latter deals with iteroparous as well as semelparous Leslie matrix models with both few and many age classes and discusses the fundamental difference among the dynamical outcomes. In recent years, there has been a growing interest of semelparous Leslie matrix models. Except for tiny parameter regions, one does not find any stable equilibria where all age classes are populated in such models. Instead, single year class (SYC) dynamics dominates where the whole population is in one age class only at each time. Papers [6–10] focus on bifurcations, SYC

dynamics as well as ergodic properties, and the dynamics and remarkable periodicity of Magicicada species has been scrutinized in [11, 12] by use of semelparous models.

In stage-structured models, which are mainly 2-dimensional, vital rates such as sexual maturity may be linked to other factors than age, for example, size, length, or weight. Among studies where stage-structured models are incorporated, we find in [13] a discussion of dynamical consequences of different density depending rates. Conditions for a population to be permanent (i.e., neither to go extinct nor explode) are considered in [14], and in [15], the authors present a numerical analysis of bifurcations in a stage-structured cannibalism model which is applied to the northeast arctic cod stock. Referring to [16], the authors show that 3-dimensional stage-structured models are not only capable of describing but also predicting chaotic behaviour in laboratory insect populations.

Turning to multispecies interactions, discrete prey-predator models of the form $x_{t+1} = f(x_t, y_t)x_t$, $y_{t+1} = g(x_t, y_t)y_t$, where x is prey and y predator, have been extensively studied from different perspectives, as accounted for in several papers. In [17], it is shown that predator populations may become extinct through subcritical bifurcations. The 4-dimensional models presented in [18] incorporate recruitment functions of both Ricker and Beverton and Holt type, and it is shown that possible periodic dynamics of low period, either exact or approximate, may not be generated by the predator, but it may be generated by the prey. In [19] the authors apply Holling type II response, while [20] considers prey-predator interactions including Allé effects. Such models often possess three equilibria (or fixed points) which correspond to (i) extinction of both species, (ii) survival of the prey and extinction of the predator, or (iii) survival of both species. The dynamics found in such systems strongly depends on compensatory or overcompensatory recruitment. In recent years, the question of how to control and stabilize chaotic behaviour in prey-predator systems has also been addressed, see [21–24] and references therein.

The purpose of this article is twofold. In one direction, we shall study two stage-structured one-population models (prey models) with varying degree of density dependence incorporated. Among our results found here are that we provide new insight of what happens at bifurcation threshold. Indeed, when the fecundity of the prey depends on the total population, we prove that the transition from stability to instability goes through a supercritical flip bifurcation in most of parameter space, but in contrast to what is found in most other population models, we also prove that there exist parameter regions where the bifurcation is of subcritical nature. If the fecundity depends on the mature part of the population only, we prove that the fixed point of model undergoes a supercritical Neimark-Sacker bifurcation at threshold. By use of the results above, we thereby show how the dynamics of (prey) species who possess a large number of different life histories may vary, and we also show that population models where the whole population contributes to density effects in general have better stability properties than models where only the mature part contributes.

In another direction, we shall study the impact of predation. The stage-structured models referred to above shall now be considered as prey, and our goal is to reveal dynamical consequences of predation and possible extinction of species where (i) the immature subpopulation of the prey is exposed to predation and (ii) the mature part of the target population. Among our findings of this study is that, depending on predation skill and life history of prey, increased predation may act both in a stabilizing and destabilizing fashion and in the latter case give birth to a great variety of dynamical outcomes.

The plan of the paper is as follows: in Section 2, we present the prey models and analyze equilibria, stability, and dynamical behaviour. In Section 3, we introduce the predator and study the impact of predation by use of four different models. Finally, in Section 4, we summarize and conclude.

2. The Prey Models

Let $x_{1,t}$ and $x_{2,t}$ be the immature and mature part of a prey population at time t , and let μ_1 and μ_2 , $0 < \mu_1, \mu_2 < 1$, be the fractions of x_1 and x_2 , respectively, that survive from time t to time $t + 1$. Moreover, we assume that p , $0 < p < 1$, is the fraction of the immature population which survives to become mature one time unit (year) later. $f = Fe^{-x}$, where $x = x_1 + x_2$ (model 1), $f = Fe^{-x_2}$ (model 2), $F > 0$, is the density dependent fecundity. Depending on the species under consideration, the terms e^{-x} and e^{-x_2} may be linked to cannibalistic behaviour, crowding effects, or other effects such that $f'(x) < 0$, $f'(x_2) < 0$. Then, see [15] or [25], we may express the relationship between x_1 and x_2 at two consecutive time steps through the models:

$$\begin{aligned} \text{Model 1: } (x_1, x_2) \mapsto \\ (\mu_1(1-p)x_1 + Fe^{-x}x_2, \mu_1px_1 + \mu_2x_2), \end{aligned} \quad (1)$$

$$\begin{aligned} \text{Model 2: } (x_1, x_2) \mapsto \\ (\mu_1(1-p)x_1 + Fe^{-x_2}x_2, \mu_1px_1 + \mu_2x_2). \end{aligned} \quad (2)$$

Although the models look pretty similar, there is a substantial difference between the dynamical outcomes. Model 1 was first proposed by Neubert and Caswell, see [13].

Both map (1) and (2) cover species with a great variety of different life histories. If $\mu_2 \rightarrow 0$, the population is semelparous (i.e., reproducing only once). Whenever $0 < \mu_2 < 1$, the population is iteroparous (repeated reproduction). $\mu_2 \rightarrow 0$ and $p \rightarrow 1$ mean that individuals face a rapid development with only one reproduction. In this case, one says that the population exhibits a precocious semelparous life history. Standard examples may be found between biennials and annual plants. Delayed semelparity occurs when $\mu_2 \rightarrow 0$ and $0 < p < 1$. Typical examples are periodical insects and salmon species which live for many years before they become mature and then reproduce only once. If $0 < \mu_2 < 1$ and $p \rightarrow 1$, the population is said to incorporate precocious iteroparous life history. Here, we find several mammals species which start to reproduce at a young age and may survive to reproduce for several years.

Excellent examples are small rodent populations. Delayed iteroparity is characterized by $0 < \mu_2 < 1$ and $0 < p < 1$. Species who belong to this subclass may live for several years in the immature stage before they reach maturity and then survive to reproduce for many years. Large mammals and humans belong to this subclass. Hence, map (1) and (2) may be used to capture the dynamics of a wide range of different (prey) populations.

We shall now reveal the dynamical properties of map (1) and map (2), and we start by map (1). Besides the trivial fixed point $(\tilde{x}_1, \tilde{x}_2) = (0, 0)$, map (1), as shown in [13], also possesses a nontrivial fixed point

$$(x_1^*, x_2^*) = \left(\frac{1 - \mu_2}{1 + \mu_1 p - \mu_2} x^*, \frac{\mu_1 p}{1 + \mu_1 p - \mu_2} x^* \right), \quad (3)$$

where

$$x^* = \ln \left(\frac{\mu_1 p F}{(1 - \mu_2)(1 - \mu_1(1 - p))} \right) = \ln R_0. \quad (4)$$

In order for (3) to be a feasible fixed point, we must assume that the inherent reproductive number R_0 exceeds unity. If $R_0 \leq 1$, it is straightforward by stability analysis to show that $(\tilde{x}_1, \tilde{x}_2)$ is stable. Therefore, $R_0 > 1$ both ensures that $(\tilde{x}_1, \tilde{x}_2)$ is repeller and that (x_1^*, x_2^*) is feasible. Moreover, we have the following result regarding map (1):

Theorem 1. *Under the assumption $R_0 > 1$, map (1) is permanent.*

Proof. To this end, writing map (1) in the form

$$x_{t+1} = A_x x_t, \quad (5)$$

where

$$\begin{aligned} \underline{x} &= (x_1, x_2)^T, \\ A_x &= \begin{pmatrix} \mu_1(1-p) & Fe^{-x} \\ \mu_1 p & \mu_2 \end{pmatrix}. \end{aligned} \quad (6)$$

Our first observation is that the restrictions on parameters and function in (1), (5) ensure that A_0 is irreducible and that A_x is nonnegative for all $(x_1, x_2) \in \mathbb{R}_+^2$. Hence, map (1), or (4), is $\mathbb{R}_+^2 / \{0\}$ forward invariant. It remains to show that there exists a compact set $X \subset \mathbb{R}_+^2$ such that for all $x \in \mathbb{R}_+^2$, there exists $t^M = t^M(x)$ satisfying $x \in X$ for all $t \geq t^M$. Now, assume $e^{-x_i} x_{2,t} \leq K_0$. Then, $x_{1,t+1} \leq \mu_1(1-p)x_{1,t} + FK_0$ and by induction

$$x_{1,t+1} \leq (\mu_1(1-p))^t x_{1,0} + \frac{FK_0}{1 - \mu_1(1-p)}. \quad (7)$$

Then, there exists $t^A = t^A(x_{1,0})$ such that for $t > t^A$

$$x_{1,t} \leq \frac{2FK_0}{1 - \mu_1(1-p)} = K_1. \quad (8)$$

Further on, in case of $t > t^A$, we also have $x_{2,t+1} \leq \mu_1 p K_1 + \mu_2 x_{2,t}$ and again by induction, for $t > t^B(x_{2,0})$

$$x_{2,t} \leq \frac{2\mu_1 p K_1}{1 - \mu_2} = K_2. \quad (9)$$

Finally, take $t^M = \max(t^A, t^B)$ and $K = \max(K_1, K_2)$. Then, for $t \geq t^M$, we have $x_{1,t} \leq K$, $x_{2,t} \leq K$, and the proof is complete.

Hence, the population density will neither go to zero nor explode. Considering the nontrivial fixed point (3), it is stable whenever

$$x_F^* < \frac{2(\mu_1(1-p) + \mu_2)(\mu_1 p + 1 - \mu_2)}{(1 - \mu_2)(1 - \mu_1(1-p))(1 + \mu_2 - \mu_1 p)}, \quad (10)$$

and undergoes a flip (period doubling) bifurcation when (10) becomes an equality.

We shall now scrutinize the nature of the bifurcation in somewhat more detail. Recall that a flip bifurcation is said to be supercritical if a stable period 2-orbit is established at threshold when (x_1^*, x_2^*) fails to be stable (i.e., when (10) becomes an equality). Otherwise, it is subcritical. \square

Theorem 2. *In case of μ_1 sufficiently large (not too close to zero), the fixed point (x_1^*, x_2^*) of map (1) will undergo a supercritical flip bifurcation when (10) becomes an equality.*

Proof. From the linearized map, we find that the eigenvalues at bifurcation threshold become $\lambda_1 = -1$ and $\lambda_2 = 1 - AB/C$, where $A = \mu_1(1-p) + \mu_2$, $B = 1 + \mu_1 p - \mu_2$, and $C = 1 + \mu_2 - \mu_1 p$. Next, we define the matrix T

$$T = \begin{pmatrix} -(1 + \mu_2) & \frac{\lambda_2 - \mu_2}{\mu_1 p} \\ 1 & 1 \end{pmatrix}, \quad (11)$$

whose columns are the eigenvectors associated to λ_1, λ_2 .

Ten, after expanding the first component of (1) up to third order, applying the change of coordinates $(\hat{x}_1, \hat{x}_2) = (x_1 - x_1^*, x_2 - x_2^*)$ (in order to translate the bifurcation to the origin), together with the transformations

$$\begin{pmatrix} \hat{x}_1 \\ \hat{x}_2 \end{pmatrix} = T \begin{pmatrix} u \\ v \end{pmatrix} \Leftrightarrow \begin{pmatrix} u \\ v \end{pmatrix} = T^{-1} \begin{pmatrix} \hat{x}_1 \\ \hat{x}_2 \end{pmatrix}, \quad (12)$$

we may rewrite (1) at threshold as

$$\begin{pmatrix} u \\ v \end{pmatrix}_{t+1} = \begin{pmatrix} -1 & 0 \\ 0 & \lambda_2 \end{pmatrix} \begin{pmatrix} u \\ v \end{pmatrix}_t + DQ(u_t, v_t) \begin{pmatrix} -1 \\ 1 \end{pmatrix}, \quad (13)$$

where $D = \mu_1 p(1 + \lambda_2)$. $Q(u_t, v_t)$ consists of terms of order two and three and may be expressed as

$$\begin{aligned}
Q(u_t, v_t) &= \frac{1}{2} f x_2^* \frac{1}{(\mu_1 p)^2} (-(1 + \mu_2)u_t + Rv_t)^2 \\
&\quad - f(1 - x_2^*) \frac{1}{\mu_1 p} (-(1 + \mu_2)u_t + Rv_t)(u_t + v_t) \\
&\quad - f \left(1 - \frac{1}{2} x_2^*\right) (u_t + v_t)^2 - \frac{1}{6} f x_2^* \frac{1}{(\mu_1 p)^3} (-(1 + \mu_2)u_t + Rv_t)^3 \\
&\quad + \frac{1}{2} f(1 - x_2^*) \frac{1}{(\mu_1 p)^2} (-(1 + \mu_2)u_t + Rv_t)^2 (u_t + v_t) \\
&\quad + f \left(1 - \frac{1}{2} x_2^*\right) \frac{1}{\mu_1 p} (-(1 + \mu_2)u_t + Rv_t)(u_t + v_t)^2 + \frac{1}{2} f \left(1 - \frac{1}{3} x_2^*\right) (u_t + v_t)^3,
\end{aligned} \tag{14}$$

where $R = \lambda_2 - \mu_2$ and $f = Fe^{-x^*}$ evaluated at threshold.

The next step involves the restriction of (13) to the center manifold. To do this, we first seek (approximate) the center manifold as a graph

$$\begin{aligned}
v &= i(u) \\
&= Ku^2 + Lu^3 + O(u^4),
\end{aligned} \tag{15}$$

and by considering the two components of (13), we find that $i(u)$ satisfies the relation

$$i(-u - DQ(u, i(u))) - \lambda_2 i(u) - DQ(u, i(u)) = 0, \tag{16}$$

from which we obtain (from (15))

$$\begin{aligned}
K &= \frac{CW}{D(1 - \lambda_2)}, \\
L &= \frac{C}{D^2} \left(\frac{AW + W^2}{1 - \lambda_2} - \frac{C(3W - A)}{6} \right),
\end{aligned} \tag{17}$$

where $W = 1 + \mu_1 \mu_2 (1 - p)$.

Finally, by substituting (15) into the first component of (13), we obtain the restricted map as

$$u_{t+1} = H(u_t), \tag{18}$$

where $H(u_t)$ at bifurcation may be written as

$$\begin{aligned}
H(u_t) &= -u_t - \frac{CW}{D} u_t^2 \\
&\quad + \frac{CW}{D} \left(\frac{(A + W)(\mu_1 p + R) + (A - W)C}{D(1 - \lambda_2)} \right. \\
&\quad \left. - \frac{C(3W - A)}{6\mu_1 p W} \right) u_t^3.
\end{aligned} \tag{19}$$

Now, following [26] (Theorem 3.5.1), the bifurcation will be of supercritical nature whenever the relations

$$\frac{\partial H}{\partial F} \frac{\partial^2 H}{\partial u^2} + 2 \frac{\partial^2 H}{\partial u \partial F} \tag{20}$$

$$= \frac{\partial H}{\partial F} \frac{\partial^2 H}{\partial u^2} - \left(\frac{\partial H}{\partial u} - 1 \right) \frac{\partial^2 H}{\partial u \partial F} \neq 0,$$

$$\frac{1}{2} \left(\frac{\partial^2 H}{\partial u^2} \right)^2 + \frac{1}{3} \left(\frac{\partial^3 H}{\partial u^3} \right) > 0, \tag{21}$$

hold. Regarding the left hand side of the nondegeneracy condition (20), it may be cast in the form

$$\frac{\mu_1 p C}{AB - 2C} e^{-2AB/(1-\mu_2)(1-\mu_1(1-p))C}, \tag{22}$$

which is clearly nonzero. The left hand side of (21) becomes

$$\begin{aligned}
&\frac{2C^2 W}{D^2} \left(\mu_1 \mu_2 (1 - p) + \frac{AB}{2C} + \frac{A}{6W} \left(2 - \frac{AB}{C} \right) \right. \\
&\quad \left. + (1 - \mu_1) \frac{A + W}{AC} - \frac{(W - A)C}{AB} \right).
\end{aligned} \tag{23}$$

The fraction outside the main parenthesis is clearly positive, and the parenthesis itself, which contains only one negative term, is positive too in most of parameter space; i.e., the bifurcation is supercritical. On the other hand, in case of μ_1 sufficiently small, the main parenthesis of (23) degenerates to

$$\left(\frac{\mu_2(1 - \mu_2)}{2(1 + \mu_2)} + \frac{\mu_2}{6} \left(2 - \frac{\mu_2(1 - \mu_2)}{1 + \mu_2} \right) - 1 \right), \tag{24}$$

which is negative. Consequently, the bifurcation is subcritical whenever μ_1 is small.

Referring to Figure 1(a), we show the region in parameter space (shaded region) where the latter phenomenon occurs. Here, we do not find smooth transition from (x_1^*, x_2^*) to a stable period 2-orbit at threshold. Instead, due to the subcritical nature of the bifurcation, we observe a jump to

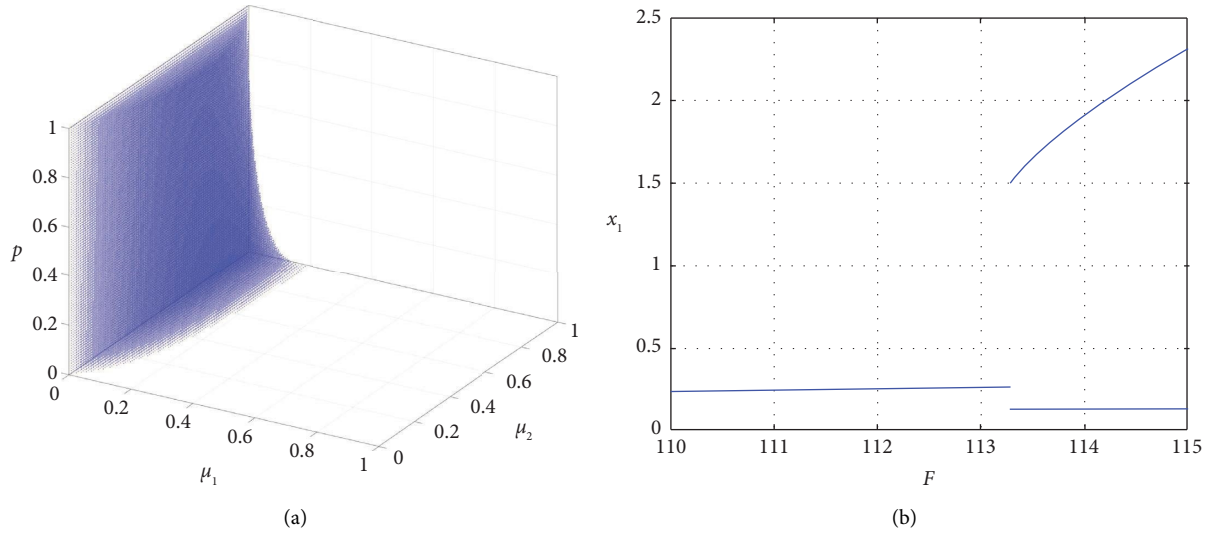


FIGURE 1: (a) Parameter space (shaded region) where the bifurcation is subcritical and (b) (x_1^*, x_2^*) undergoes a subcritical bifurcation when $F = 113.244$, parameter values $(\mu_1, \mu_2, p) = (0.05, 0.1, 0.2)$.

a 2-cycle which is created at a smaller F -value as demonstrated in Figure 1(b).

Let us now in somewhat more detail scrutinize the dynamics in the region where the bifurcation is supercritical. Our first observation, confer (10), is that the value of F (or $x^* = \ln R_0$) at instability threshold is smaller in the precocious cases compared to the delayed cases which signals that species who possess a delayed semelparous or iteroparous life history have better stability properties than species with precocious semelparous or iteroparous life histories.

In Figure 2(a), we show the bifurcation diagram generated by (1) in the precocious semelparous case $(\mu_1, \mu_2, p) = (1, 0.1, 0.9)$. At instability threshold, $F = 76.64$, and the stable period 2-orbit persists in a huge F interval

before chaos is introduced. Referring to Figure 2(b), the delayed semelparous case $(\mu_1, \mu_2, p) = (1, 0.1, 0.5)$, and the fixed point becomes unstable when $F = 453.44$ and F must exceed 1000 in order to capture chaotic dynamics. There is no sign of periodic orbits of period $2^k, k > 1$.

However, the dynamics generated by (1) may be much richer than reported above. This is due to the well-known fact that nonlinear systems may possess multiple attractors. In Figure 3(a), where we still use $(\mu_1, \mu_2, p) = (1, 0.1, 0.9)$ (precocious semelparity) but a different initial value than in Figure 2(a) we find other attractors. Indeed, whenever $F_C < F < 44.73$ where $F_C = 23.12$, the stable fixed point (x_1^*, x_2^*) coexists with a stable 3-cycle. Our conjecture is that the 3-cycle is established as the third iterate of (1) which may be expressed as

$$\begin{aligned}
 x_{1,t+3} &= (\mu_1^2(1-p)(\mu_1(1-p)^2 + pFe^{-A_1}) + \mu_1 pF(\mu_1(1-p) + \mu_2)e^{-A_2})x_{1,t} \\
 &\quad + (\mu_1(1-p)F(\mu_1(1-p)e^{-x_t} + \mu_2e^{-A_1}) + (\mu_1 pFe^{-x_t} + \mu_2^2)Fe^{-A_2})x_{2,t}, \\
 x_{2,t+3} &= (\mu_1^3 p(1-p)^2 + \mu_1^2 \mu_2 p(1-p) + \mu_1 \mu_2^2 p + \mu_1^2 p^2 Fe^{-A_1})x_{1,t} \\
 &\quad + (\mu_1 pF(\mu_1(1-p) + \mu_2)e^{-x_t} + \mu_1 \mu_2 pFe^{-A_1} + \mu_2^3)x_{2,t},
 \end{aligned} \tag{25}$$

where

$$\begin{aligned}
 A_1 &= \mu_1 x_{1,t} + (Fe^{-x_t} + \mu_2)x_{2,t}, \\
 A_2 &= (\mu_1^2(1-p) + \mu_1 \mu_2 p + \mu_1 pFe^{-A_1})x_{1,t} \\
 &\quad + (\mu_1 Fe^{-x_t} + \mu_2 Fe^{-A_1} + \mu_2^2)x_{2,t},
 \end{aligned} \tag{26}$$

undergoes a saddle node bifurcation.

In order to support the conjecture, we have proved numerically that the dominant eigenvalue of the linearization of (25) evaluated at the point $(x_1, x_2) = (6.271181, 0.384385)$

(one of the points on the 3-cycle when $F = F_C$) equals $\lambda_1 = 1.000323$ ($\lambda_2 = -0.00108$). Thus, our conjecture is supported. When $F_C < F < 45$, map (25) generates 3 branches of stable fixed points and 3 branches of unstable fixed points (not visible). Actually, for a given value of F , map (25) has seven fixed points since (x_1^*, x_2^*) is a fixed point too. As F is increased, see Figure 3(a), we find coexistence between the stable fixed point (x_1^*, x_2^*) and stable cycles of period $3 \cdot 2^k, k > 1$, which are established as map (25) undergoes successive flip bifurcations. Beyond the point of accumulations for the flip bifurcation sequence, the dynamics becomes chaotic. Hence,

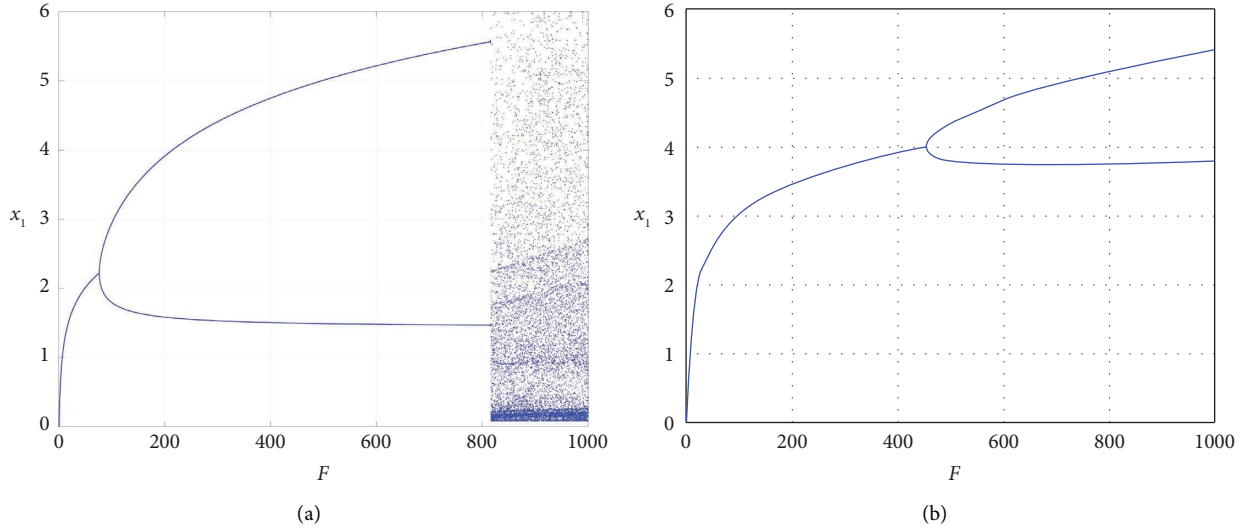


FIGURE 2: Bifurcation diagram generated by map (1): (a) $(\mu_1, \mu_2, p) = (1, 0.1, 0.9)$ and (b) $(\mu_1, \mu_2, p) = (1, 0.1, 0.5)$.

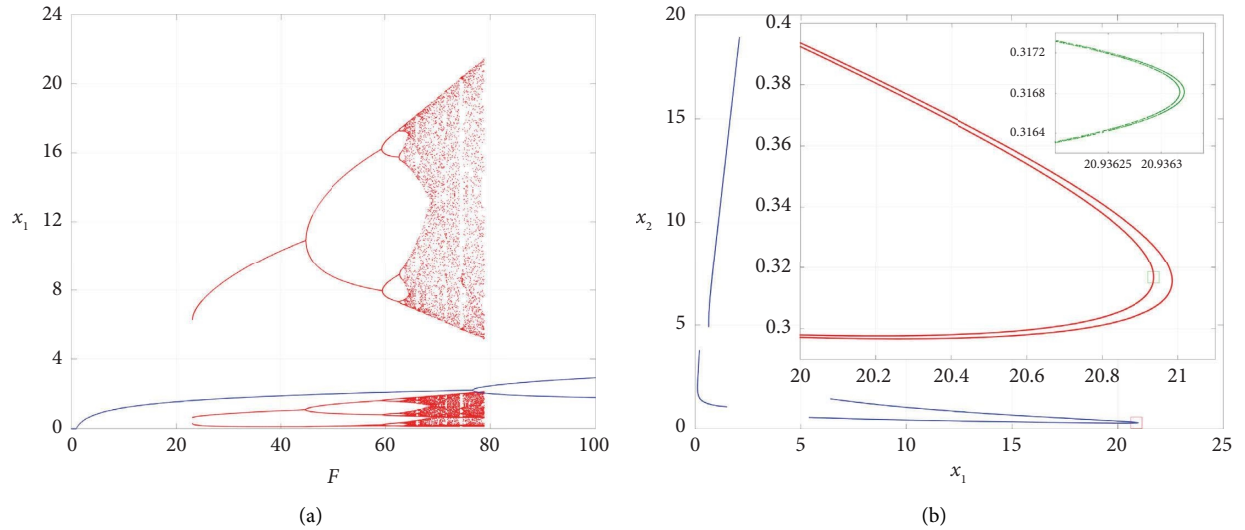


FIGURE 3: (a) Bifurcation diagram generated by map (1): parameter values $(\mu_1, \mu_2, p) = (1, 0.1, 0.9)$ and different initial values than in Figure 2(a) and (b) chaotic dynamics generated by map (1), with zooms showing fractal structure. Parameter values $(\mu_1, \mu_2, p, F) = (1, 0.1, 0.9, 77)$.

there exists an F interval where (x_1^*, x_2^*) coexists with a chaotic attractor as well. At $F = 76.6373$, (x_1^*, x_2^*) experiences a supercritical flip bifurcation which means that there is also an interval where a stable 2-cycle and the chaotic attractor coexist. The structure of the latter is shown in Figure 3(b). Hence, the ultimate fate of an orbit in this part of parameter space strongly depends on the initial conditions. The chaotic attractor disappears when $F = 78.89$. We suspect that it happens as the attractor is hit by a branch of unstable equilibria (born when $F = F_C$) generated by (25). In order to scrutinize this, see Figure 3(a), we have found numerically one of the lowest points of the upper subset of the attractor to be $(x_1, x_2) = (5.0539, 1.71103)$ and then used it as input in map (25). After one iteration, the result is $(x_{1,A}, x_{2,A}) = (5.0590, 1.7093)$, thus $(x_1, x_2) \approx (x_{1,A}, x_{2,A})$

which clearly suggests that (x_1, x_2) is a fixed point of map (25). Evidently, the point must be located at a branch of unstable equilibria.

We may also describe the dynamics by use of the maximal Lyapunov exponent L . Recall that $L < 0$ corresponds to a stable fixed point or a stable periodic orbit. $L = 0$ (which we do not find in our case) corresponds to quasi-periodic orbits restricted to an invariant curve, while $L > 0$ implies chaotic dynamics. In Figure 4(a), we show the results of computing L by use of the same values as when Figure 2(a) was generated. What the diagram shows is that whenever $F < 76.6373$, the fixed point (x_1^*, x_2^*) is stable (i.e., $L < 0$). It becomes unstable when $F = 76.6373$, and thereafter, the dynamics turns to a stable 2-orbit (i.e., $L < 0$). Referring to Figure 4(b), the F interval where $L > 0$ corresponds to

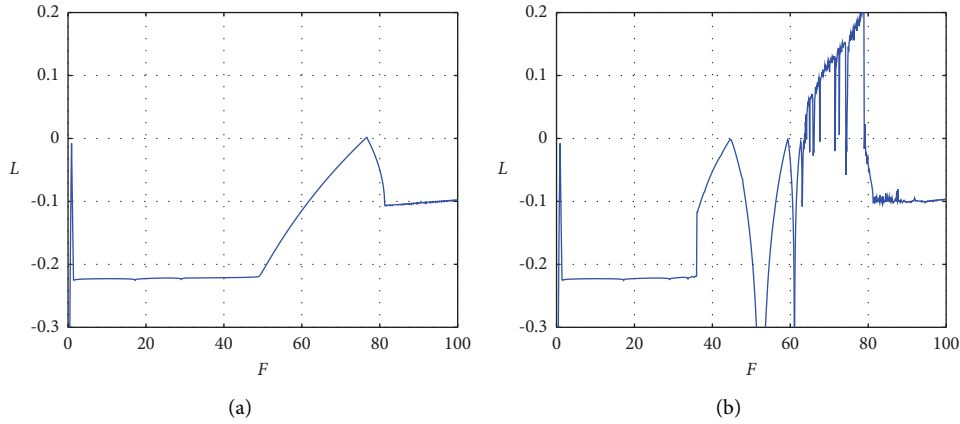


FIGURE 4: Lyapunov exponent L calculated from map (1). Parameter values $(\mu_1, \mu_2, p) = (1, 0.1, 0.9)$: (a) initial points $(x_{1,0}, x_{2,0})$ are close to (x_1^*, x_2^*) and (b) $(x_{1,0}, x_{2,0}) = (1, 1)$.

chaotic dynamics. Prior to this, we find stable $3 \cdot 2^k$, $k \geq 0$, cycles ($L < 0$), and whenever $F > 78.79$, the dynamics is 2-periodic ($L < 0$). Evidently, there is an excellent agreement between the results. Finally, as already mentioned, the fate of an orbit depends on the initial condition. In order to pinpoint where orbits starting at different initial points $(x_{1,0}, x_{2,0})$ will settle, we have computed the trapping regions for the various attractors. One such example is shown in Figure 5 where $(\mu_1, \mu_2, p, F) = (1, 0.1, 0.9, 50)$. The trapping region for the 6-cyclic attractor is the shaded part of the figure while the trapping region for the stable fixed point is the white part. Clearly, the shaded part is by far the largest. Moreover, similar computations by use of other values of F lead to much of the same qualitative picture. Hence, it is natural to conclude that in the interval $35 < F < 77$, most orbits will not settle on (x_1^*, x_2^*) , but on one of the other attractors.

Next, let us give a short description of the dynamical behaviour of species who possess other life histories. There is a fairly good resemblance between both the delayed semelparous case, the precocious iteroparous case, and the one already accounted for. For small values of F , the only attractor is the fixed point, but there are also F intervals where we find multiple attractors. For example, if $(\mu_1, \mu_2, p) = (1, 0.1, 0.5)$ (delayed semelparity), there exists an F interval where the stable fixed point coexists with a stable 3-cycle, but also F intervals $F > F_C$ where a stable 2-cycle coexists with stable 6-cycles, 12-cycles as well as a chaotic attractor. In the precocious iteroparous case, we observe much of the same qualitative picture, but chaotic dynamics appears to be absent. Regarding the last case (delayed iteroparity), we have not detected anything else than a stable fixed point, $F < F_F$, or a stable 2-cycle, $F > F_F$ (F_F is a large number).

Next, we shall focus on the dynamical properties of map (2), and in part of the analysis, we may use results obtained in [27]. The nontrivial fixed point of (2) is

$$(x_1^*, x_2^*) = \left(\frac{1 - \mu_2}{\mu_1 p}, x_2^*, x_2^* \right), \quad (27)$$

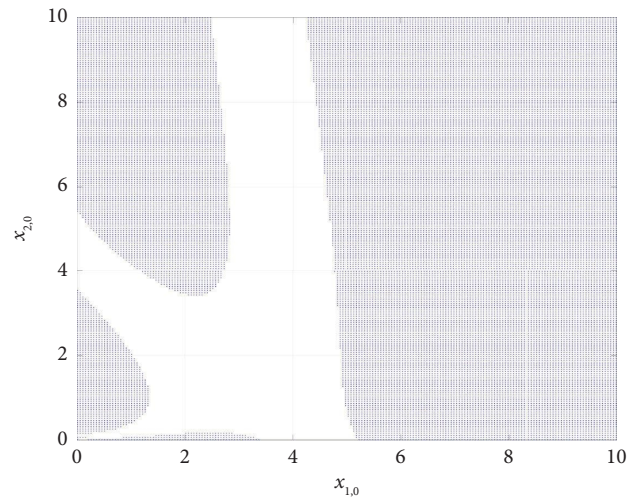


FIGURE 5: Model (1) trapping region $(\mu_1, \mu_2, p, F) = (1, 0.1, 0.9, 50)$. Shaded part is the 6-cyclic attractor, while the fixed point is white.

where

$$x_2^* = \ln \left(\frac{\mu_1 p F}{(1 - \mu_2)(1 - \mu_1(1 - p))} \right) = \ln R_0, \quad (28)$$

and we recognize that R_0 here is the same as R_0 in map (1). Moreover, $R_0 \leq 1$ implies that the origin is stable, and $R_0 > 1$ guarantees both that $(0, 0)$ is a repeller, (x_1^*, x_2^*) is feasible, and that map (2) is permanent.

From the linearization of (2) and the Jury criteria, it follows that (x_1^*, x_2^*) is a stable fixed point provided

$$x_2^* < \frac{2(\mu_1(1 - p) + \mu_2)}{(1 - \mu_2)(1 - \mu_1(1 - p))} = x_{2C}. \quad (29)$$

Criterion (29), $x_2^* < x_{2C}$ clearly holds in case of small values of R_0 , but when R_0 is increased (as a result of increasing F), $\ln R_0$ becomes equal to x_{2C} which is equivalent to say

$$F = F_C = \frac{(1-\mu_2)(1-\mu_1(1-p))}{\mu_1 p} e^{2-(\mu_1(1-p)+\mu_2)/(1-\mu_2)(1-\mu_1(1-p))}. \quad (30)$$

This happens as a pair of complex valued eigenvalues cross the unit circle. Hence, in contrast to fixed point (3), fixed point (28) undergoes a Neimark-Sacker bifurcation at instability threshold (30). Regarding the nature of bifurcation (supercritical or subcritical), we have the following result: \square

Theorem 3. *The fixed point (28) of map (2) undergoes a supercritical Neimark-Sacker bifurcation at threshold (30).*

Proof. Following the procedure outlined in [26], it is possible to rewrite (2) at bifurcation threshold as

$$\begin{pmatrix} u \\ v \end{pmatrix} \mapsto \begin{pmatrix} \operatorname{Re}\lambda & -\operatorname{Im}\lambda \\ \operatorname{Im}\lambda & \operatorname{Re}\lambda \end{pmatrix} \begin{pmatrix} u \\ v \end{pmatrix} + \begin{pmatrix} 0 \\ g(u) \end{pmatrix}, \quad (31)$$

where

$$\begin{aligned} \operatorname{Re}\lambda &= \frac{\mu_1(1-p) + \mu_2}{2}, \\ \operatorname{Im}\lambda &= \frac{\sqrt{4 - (\mu_1(1-p) + \mu_2)^2}}{2} = \frac{b}{2}, \end{aligned} \quad (32)$$

$$\begin{aligned} g(u) &= -\frac{1}{b}Mu^2 - \frac{1}{3b}Nu^3, \\ M &= \mu_1(1-p) + \mu_2 - 2\mu_1(1-p)\mu_2, \\ N &= 1 - 2\mu_1(1-p) - 2\mu_2 + 3\mu_1(1-p)\mu_2. \end{aligned} \quad (33)$$

By use of Theorem 3.5.2 in [26], it now follows that the stability coefficient a may be expressed as

$$a = -\frac{1}{16} \left(\left(\frac{M}{b} \right)^2 (\mu_1(1-p) + \mu_2 + 6) + N \right). \quad (34)$$

Clearly, $a < 0$ and since

$$\frac{d}{dF} |\lambda| = \frac{1}{2} \mu_1 p e^{-2-(\mu_1(1-p)+\mu_2)/(1-\mu_2)(1-\mu_1(1-p))}, \quad (35)$$

(evaluated at threshold) means that the eigenvalues leave the unit circle, and we conclude that the Neimark-Sacker bifurcation is supercritical.

Thus, in contrast to our findings from map (1), when equilibrium point (27) fails to be stable, an attracting invariant curve is established for $F > F_C$ and $|F - F_C|$ small.

Our next goal is to scrutinize the dynamics in somewhat more detail. In order to compare with the findings from map (1), we concentrate on the $(\mu_1, \mu_2, p) = (1, 0.1, 0.9)$ case (precocious semelparity). Figure 6(a) shows the bifurcation diagram generated by map (2) in the F range $5 < F < 50$, and in Figure 6(b), we show computations of the Lyapunov exponent L . The fixed point is stable for F values less than 8.305 (confer (30)). In the interval $8.305 < F < 15.5$, we find the invariant curve, see Figure 7(a), which is followed by a short interval where the dynamics becomes chaotic ($L > 0$). If we continue to increase F , the dynamics turns periodic, first 8-periodic, then 4-periodic, see Figure 7(b), before it again becomes chaotic. Note that the points in the 8-cycles are clustered in such a way that one from an observational point of view probably will classify the dynamics as almost 4-periodic, and the same argument also applies in the ‘‘chaotic’’ situation displayed in 7(c). Hence, we conclude that there exists a large parameter interval where the dynamics has a great resemblance of 4-cycles, either exact or approximate.

Finally, consider species with different life histories (delayed semelparous, precocious iteroparous, or delayed iteroparous). In all these cases, the dynamics beyond instability threshold is quite similar. Indeed, except for tiny parameter windows where we find periodic orbits of long period, the dynamics is nonperiodic and restricted to attracting invariant curves. There is no sign of chaotic behaviour. The main difference is the value of F at threshold which is much larger in the delayed cases compared to the precocious cases which also implies that $x^* = x_1^* + x_2^*$ is significantly larger. Hence, the results obtained above confirm findings in [13] or [25], namely that species with delayed semelparous or iteroparous life histories have better stability properties than species with precocious semelparous or iteroparous life histories. \square

3. Predation

We shall now turn to the impact of predation, and the analysis will be confined to four different cases. In two of the cases (cases I and III), it will be assumed that only the immature part of the prey population is exposed to predation, while cases II and IV treat the situation where the mature part of the prey population is the target. The models we shall apply are as follows:

$$\text{Case I: } (x_1, x_2, y) \mapsto ((\mu_1(1-p)x_1 + Fe^{-x_2}x_2)e^{-ay}, \mu_1px_1 + \mu_2x_2, c(\mu_1(1-p)x_1 + Fe^{-x_2}x_2)(1 - e^{-ay})), \quad (36)$$

$$\text{Case II: } (x_1, x_2, y) \mapsto (\mu_1(1-p)x_1 + Fe^{-x_2}x_2, (\mu_1px_1 + \mu_2x_2)e^{-ay}, c(\mu_1px_1 + \mu_2x_2)(1 - e^{-ay})), \quad (37)$$

$$\text{Case III: } (x_1, x_2, y) \mapsto ((\mu_1(1-p)x_1 + Fe^{-x}x_2)e^{-ay}, \mu_1px_1 + \mu_2x_2, c(\mu_1(1-p)x_1 + Fe^{-x}x_2)(1 - e^{-ay})), \quad (38)$$

$$\text{Case IV: } (x_1, x_2, y) \mapsto (\mu_1(1-p)x_1 + Fe^{-x}x_2, (\mu_1px_1 + \mu_2x_2)e^{-ay}, c(\mu_1px_1 + \mu_2)(1 - e^{-ay})). \quad (39)$$

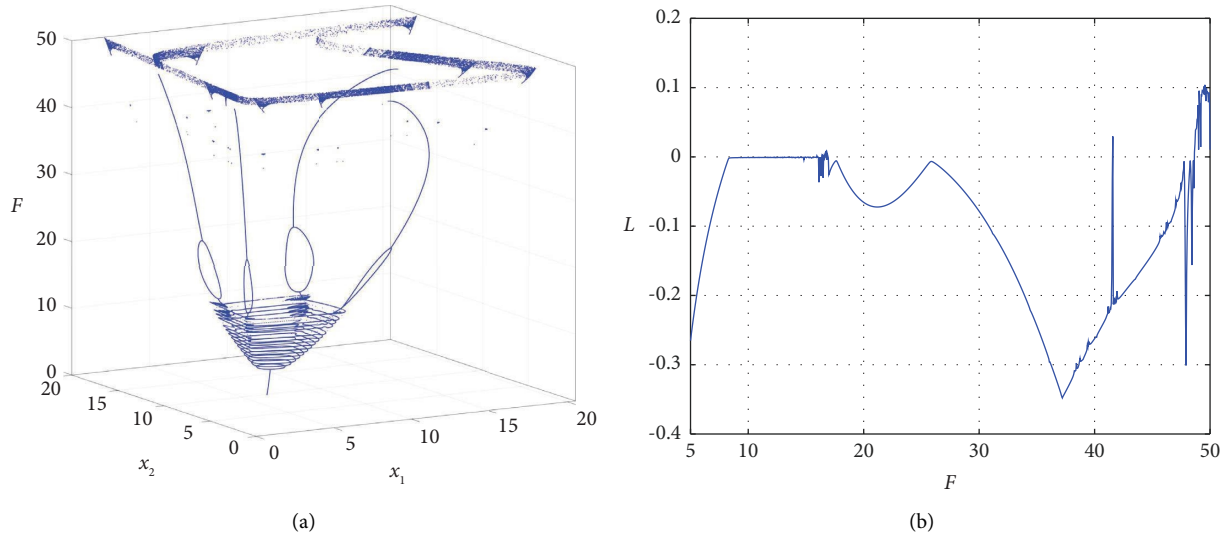


FIGURE 6: (a) Bifurcation diagram generated by map (2), $(\mu_1, \mu_2, p) = (1, 0.1, 0.9)$ and (b) Lyapunov exponent values L calculated from map (2), $(\mu_1, \mu_2, p) = (1, 0.1, 0.9)$.

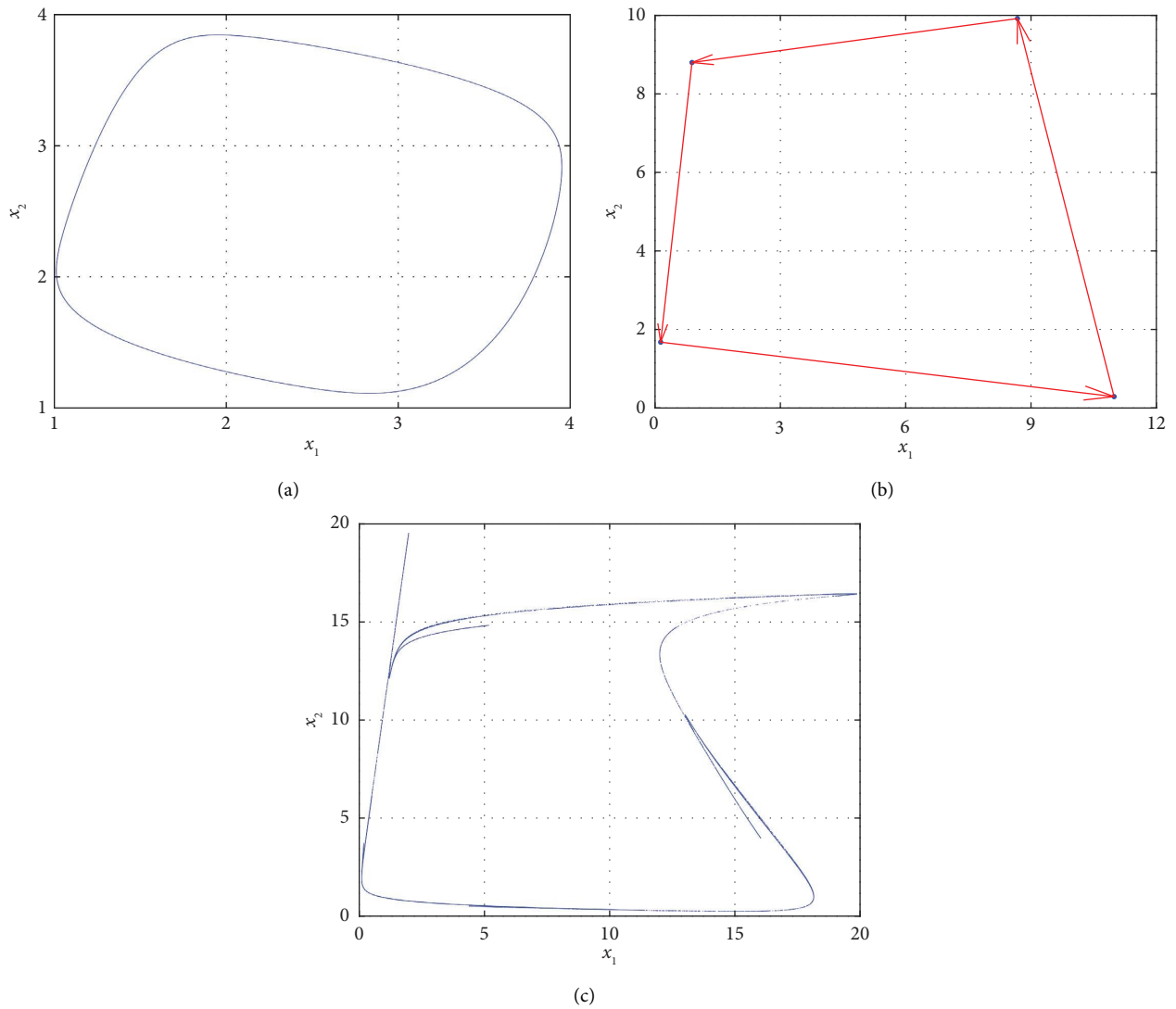


FIGURE 7: Dynamics generated by map (2). Parameter values $(\mu_1, \mu_2, p) = (1, 0.1, 0.9)$: (a) $F = 10$, (b) $F = 35$, and (c) $F = 49$.

In (36)–(39), x_1 , x_2 , μ_1 , μ_2 , p , and F have the same meaning as in map (1) and map (2). y denotes the size of the predator population and predation is accounted for by the term e^{-ay} . Parameter a , $a \geq 0$, measures the skill of predation. The constant c , $0 < c \leq 1$, may be interpreted as a conversion of prey into predator, or a clutch parameter the following year, confer [27] or [28]. Note that when $a \rightarrow 0$ (poor predation skill), the predator will die, and maps (36)–(39) will degenerate to map (1) or map (2). Biologically, models I and III may apply to interacting fish populations where small individuals of one species are exposed to cannibalism from mature relatives as well as predation from another species. Models II and IV deal with situations where mature members of a species migrate to other habitats in order to spawn and subsequently become vulnerable to predation.

Evidently, (36)–(39) share several common features. All maps possess two fixed points, the trivial one $(\hat{x}_1, \hat{x}_2, \hat{y}) = (0, 0, 0)$ and the nontrivial one (x_1^*, x_2^*, y^*) . The latter may be on the form $(x_1^*, x_2^*, 0)$ if the skill parameter a falls below a certain threshold a_C , or if the clutch parameter c becomes too small. Stability properties are found from the

linearizations of (36)–(39). All associated eigenvalue equations are on the form

$$\lambda^3 + a_1\lambda^2 + a_2\lambda + a_3 = 0. \quad (40)$$

The various fixed points will be stable if all eigenvalues of (40) are located within the unit circle which is ensured whenever the Jury criteria

$$1 + a_1 + a_2 + a_3 > 0, \quad (41a)$$

$$1 - a_1 + a_2 - a_3 > 0, \quad (41b)$$

$$1 - |a_3| > 0, \quad (41c)$$

$$|1 - a_3^2| - |a_2 - a_3a_1| > 0, \quad (41d)$$

hold. We start by considering Case I, map (36), i.e., the case where only the mature part x_2 of the prey population contributes to density effects and only the immature part x_1 is exposed to predation. The nontrivial fixed point may be expressed as

$$(x_1^*, x_2^*, y^*) = \left(\frac{1 - \mu_2}{\mu_1 p} \ln \left(\frac{\mu_1 p F}{(1 - \mu_2)(e^{ay^*} - \mu_1(1 - p))} \right), \ln \left(\frac{\mu_1 p F}{(1 - \mu_2)(e^{ay^*} - \mu_1(1 - p))} \right), y^* \right), \quad (42)$$

where y^* must be found by means of numerical methods from

$$y^* = c(e^{ay^*} - 1) \frac{1 - \mu_2}{\mu_1 p} \ln \left(\frac{\mu_1 p F}{(1 - \mu_2)(e^{ay^*} - \mu_1(1 - p))} \right). \quad (43)$$

When the skill parameter a is less than a_C , there is no value $y^* > 0$. Hence, $(x_1^*, x_2^*, y^*) \rightarrow (x_1^*, x_2^*, 0)$ where the values of x_1^* , x_2^* are found from (27). However, when $a > a_C$ and $|a - a_C|$ are small, one detects significant changes. We observe an abrupt reduction of x_1^* , x_2^* values while the value

of y^* grows. These scenarios are displayed in Figure 8 where it is assumed that the prey population possesses a precocious semelparous life history. In Figure 8(a), $F = 5$ which implies that (x_1^*, x_2^*) is stable in the absence of predation. Referring to Figure 8(b), $F = 15$ which means that (x_1^*, x_2^*) is unstable.

The analysis above does not address the question of dynamical behaviour, but as we have seen, an increase of the skill parameter plays a crucial role; hence, it is natural to suspect profound dynamical consequences as well. In order to capture these, we must turn to the linearization of map (36) and the corresponding Jury criteria (41a)–(41d) which may be cast in the form

$$J_1(a) = (1 - \mu_2)(1 - acx_1^*) + (acx_1^* - e^{-ay^*}) \cdot (\mu_1 p B_1 + \mu_1(1 - p)(1 - \mu_2)) > 0, \quad (44a)$$

$$J_2(a) = (1 + \mu_2)(1 + acx_1^*) + (acx_1^* + e^{-ay^*}) \cdot (\mu_1(1 - p)(1 + \mu_2) - \mu_1 p B_1) > 0, \quad (44b)$$

$$J_3(a) = 1 - acx_1^* |\mu_1 p B_1 - \mu_1(1 - p)\mu_2| > 0, \quad (44c)$$

$$J_4(a) = \left| 1 - (acx_1^*)^2 (\mu_1 p B_1 - \mu_1(1 - p)\mu_2)^2 \right| - \left| acx_1^* (\mu_1(1 - p) + \mu_2) + (\mu_1 p B_1 - \mu_1(1 - p)\mu_2) \right. \\ \left. \cdot ((acx_1^*)^2 + acx_1^* (\mu_1(1 - p)e^{-ay^*} + \mu_2) - e^{-ay^*}) \right| > 0, \quad (44d)$$

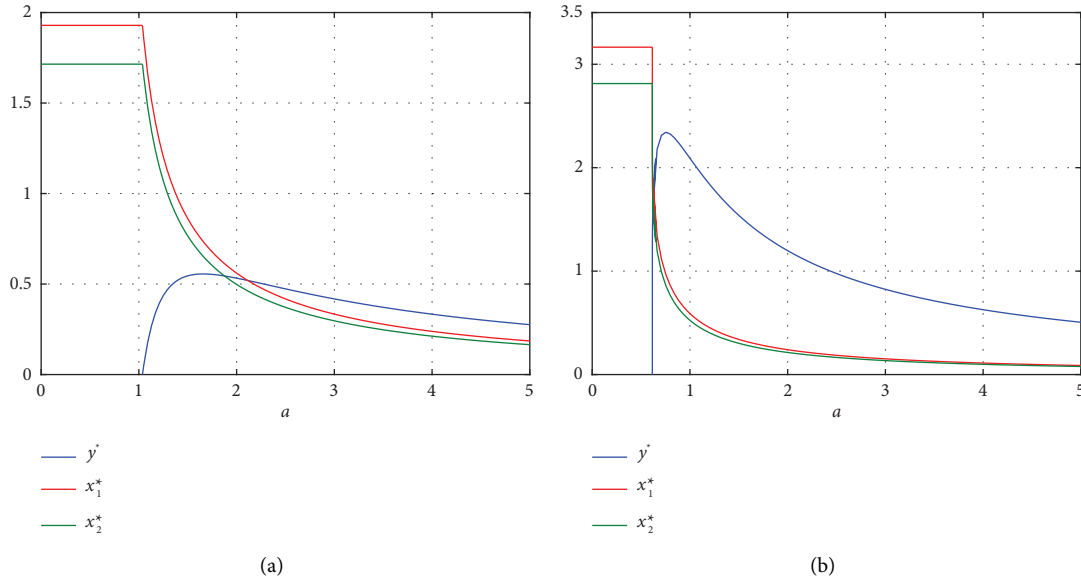


FIGURE 8: Values of x_1^* , x_2^* and y^* as functions of skill parameter a . Parameter values: $(\mu_1, \mu_2, p, c) = (1, 0.1, 0.8, 0.5)$: (a) $F = 5$ and (b) $F = 15$.

where

$$B_1 = Fe^{-x_2^*} (1 - x_2^*). \quad (45)$$

Alternatively by use of

$$\begin{aligned} x_1^* &= \frac{y^*}{c(e^{ay^*} - 1)}, \\ x_2^* &= \frac{\mu_1 p}{1 - \mu_2} x_1^*, \\ Fe^{-x_2^*} &= \frac{1 - \mu_2}{\mu_1 p} (e^{ay^*} - \mu_1(1 - p)), \end{aligned} \quad (46)$$

one may express (44a)–(44d) in terms of y^* only.

If all four inequalities hold, (x_1^*, x_2^*, y^*) is stable. When (44a) or (44b) fail to be positive, this corresponds to the case where the dominant eigenvalue of (40) leaves the unit circle through 1 or -1 , respectively, while (44c) and (44d) fail as a pair of complex valued eigenvalues leave the unit circle.

Now, considering prey species who possess semelparous life histories (precocious or delayed), the impact of predation on the immature subpopulation is as follows: whenever F is small enough for (x_1^*, x_2^*) to be stable in absence of predation, we always find a skill parameter interval $a_C < a < a_m$ where (x_1^*, x_2^*, y^*) is stable. The interval becomes smaller as F is increased. The transfer from stability to instability

occurs when $J_4(a)$ becomes zero at $a = a_m$. This is displayed in Figure 9(a) by use of the same parameters as in Figure 8(a). If (x_1^*, x_2^*) is unstable in lack of predators (larger F values), confer Figure 9(b), there exists an additional interval $a_C < a < a_{C_1}$ where the dynamics is quasiperiodic and restricted to an invariant curve. Through further increase of a , it follows an interval $a_{C_1} < a < a_m$ where (x_1^*, x_2^*, y^*) is stable. Beyond threshold a_m (both in case of small and larger F values), there are quasiperiodic orbits whenever $|a - a_m|$ is small. For larger values of a , the dynamics alternates between chaotic and periodic dynamics of long period. The larger the F , the larger the chaotic region. These scenarios are visualized in the Lyapunov exponent diagrams, Figures 10(a) and 10(b). Turning to species who possess an iteroparous life history, the impact of predation on dynamics appears to be quite similar. The main difference really is that the skill parameter interval where the fixed point (x_1^*, x_2^*, y^*) is stable is larger than in the precocious semelparous case, and the same applies in the delayed cases. Moreover, for fixed values of F and small values of a , the subpopulations x_1^*, x_2^* as well as y^* are in general larger in the iteroparous cases.

Next, let us comment on Case II, map (37), i.e., the case where the mature part of the prey population is exposed to harvest. The fixed point of map (37) may be expressed as

$$(x_1^*, x_2^*, y^*) = \left(\frac{e^{ay^*} - \mu_2}{\mu_1 p} \ln \left(\frac{\mu_1 p F}{(1 - \mu_1(1 - p))(e^{ay^*} - \mu_2)} \right), \ln \left(\frac{\mu_1 p F}{(1 - \mu_1(1 - p))(e^{ay^*} - \mu_2)} \right), y^* \right), \quad (47)$$

where y^* must be obtained from

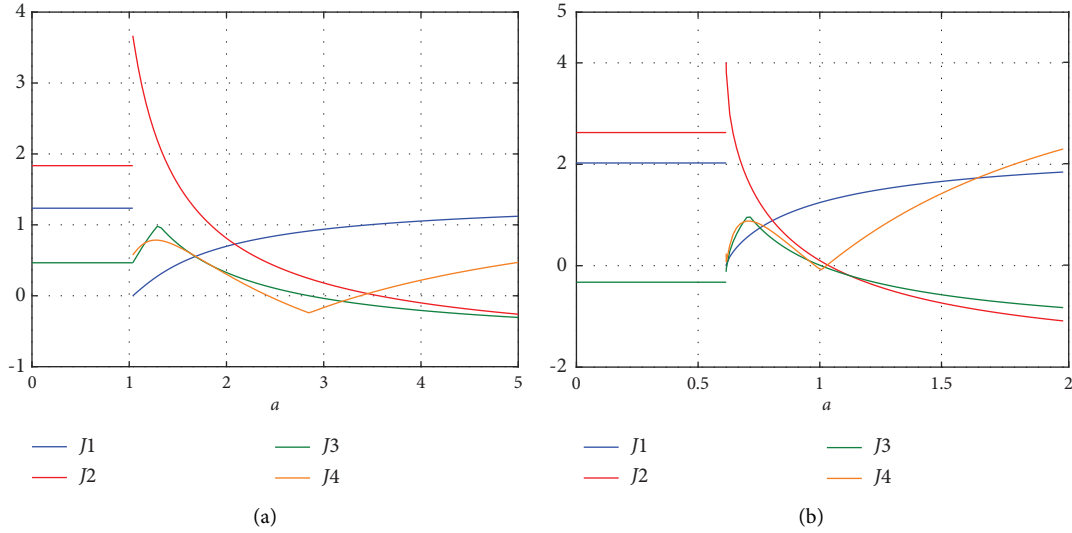


FIGURE 9: Jury criteria $J_1(a), \dots, J_4(a)$ as functions of a : (a) $F = 5$ and $a_C = 1.0369$ and (b) $F = 15$ and $a_C = 0.61357$. (The horizontal lines to the left of a_C represent the Jury criteria, and we find from the pure prey map (27)).

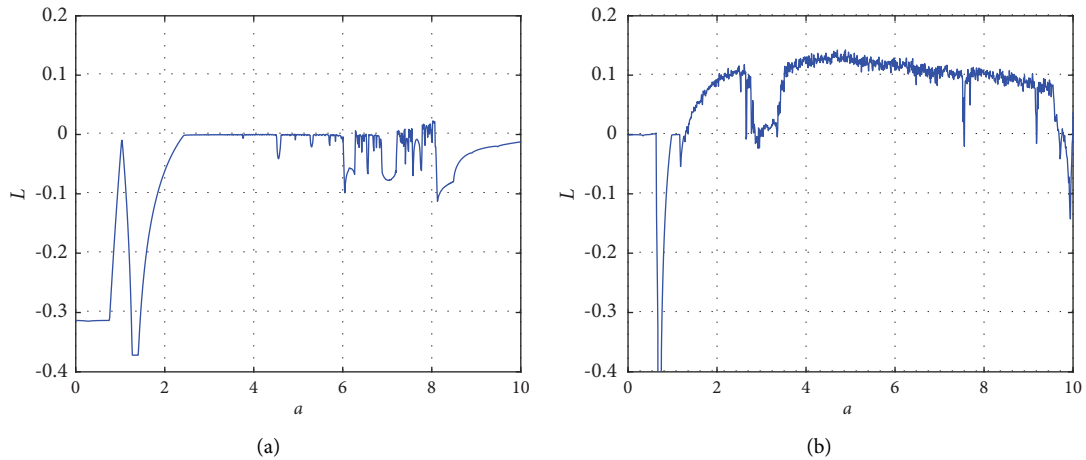


FIGURE 10: Lyapunov exponent values L calculated from map (36). Parameter values (a) $(\mu_1, \mu_2, p, F, c) = (1, 0.1, 0.8, 5, 0.5)$ and (b) $(\mu_1, \mu_2, p, F, c) = (1, 0.1, 0.8, 15, 0.5)$.

$$y^* = c(e^{ay^*} - 1) \ln \left(\frac{\mu_1 p F}{(1 - \mu_1(1 - p))(e^{ay^*} - \mu_2)} \right). \quad (48)$$

Stability and dynamic behaviours are scrutinized in the same manner as in Case I. Therefore, we skip calculation formulae in the text and go directly to the results. In Figures 11(a) and 11(b), we show the graphs of x_1^*, x_2^*, y^* and the Jury criteria J_1, \dots, J_4 as functions of a , respectively. Referring to Figure 11(a), we find, in contrast to Case I, that when $a > a_C$ and $|a - a_C|$ is small, an enlargement of a results in a larger subpopulation x_1^* . The rationale behind this is as follows: when the predator is capable of catching grown up individuals, the size of x_2^* drops which in turn implies that the strength of negative effects on recruitment at equilibrium (cannibalism, crowding effects, etc.) becomes smaller. Thus, the term $e^{-x_2^*}$ will be larger than it would be in the

absence of predation. Therefore, as long as x_2^* does not drop too much, the term $F e^{-x_2^*} x_2^*$ will increase, and the larger the F , the larger is the effect. When parameter a exceeds a certain threshold, x_1^* becomes smaller too but we emphasize that the values of x_1^* in general are much larger than in Case I. Referring to Figure 11(b), we also here find an interval $a_C < a < a_m$ where fixed point (47) is stable, and just as in Case I, (x_1^*, x_2^*, y^*) loses its hyperbolicity when $J_4(a)$ becomes zero. Hence, at threshold, (x_1^*, x_2^*, y^*) undergoes a Neimark-Sacker bifurcation. Independent of life history, when $a > a_m$, it is possible to obtain quasiperiodic behaviour, periodic orbits of long periods as well as chaotic dynamics. However, we have revealed one difference between the dynamics of species who possess semelparous and iteroparous life histories. Suppose that F is so large that (x_1^*, x_2^*) is unstable in the absence of predation. Then, in the semelparous cases, there exists a values less than a_C such that

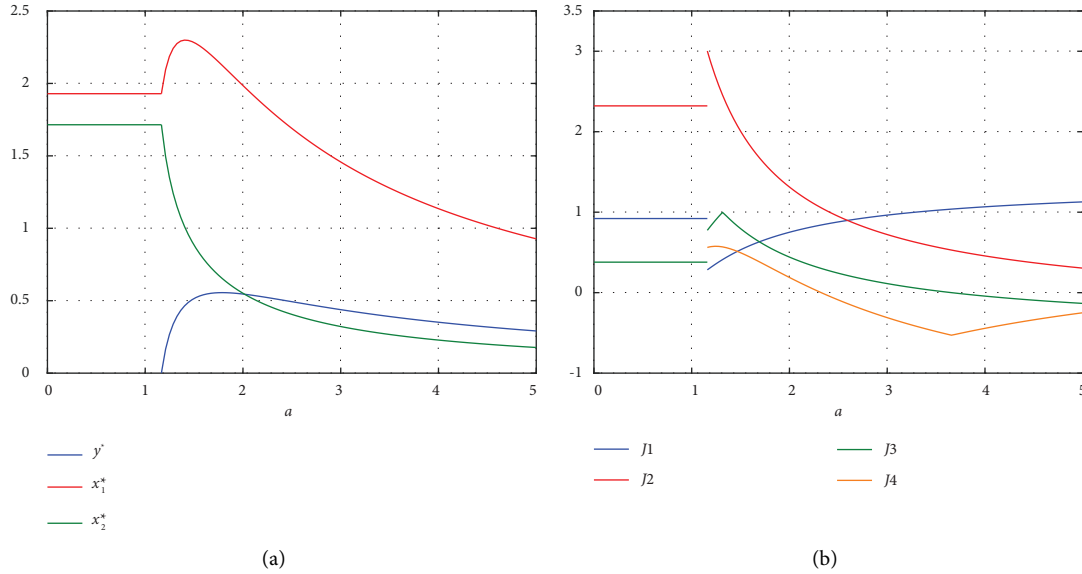


FIGURE 11: (a) Values of x_1^* , x_2^* and y^* as functions of skill parameter a , map (37). (b) Jury criteria, $J_1(a), \dots, J_4(a)$, map (37). Parameter values $(\mu_1, \mu_2, p, F, c) = (1, 0.1, 0.8, 5, 0.5)$.

the dynamics occurs on an invariant curve where $y = 0$. On the other hand, in the iteroparous case, the y values on such a curve is larger than zero confer Figures 12(a) and 12(b).

Let us now focus on the remaining cases III and IV (maps (38) and (39)), the cases where the whole prey population contributes to density effects, not the mature

subpopulation only. Moreover, recall that when $a \rightarrow 0$, maps (38) and (39) degenerate to map (1), and at bifurcation threshold (5), the value of F is much larger than in the corresponding map (2) which is the underlying prey model of maps (36) and (37). Regarding case III, map (38) where the immature part of the prey is exposed to predation we find

$$(x_1^*, x_2^*, y^*) = \left(\frac{1 - \mu_2}{1 + \mu_1 p - \mu_2} \ln \left(\frac{F \mu_1 p}{(1 - \mu_2)(e^{a y^*} - \mu_1(1 - p))} \right), \frac{\mu_1 p}{1 + \mu_1 p - \mu_2} \ln \left(\frac{F \mu_1 p}{(1 - \mu_2)(e^{a y^*} - \mu_1(1 - p))} \right), y^* \right), \quad (49)$$

where y^* must be found by means of numerical methods from

$$y^* = c \frac{1 - \mu_2}{1 + \mu_1 p - \mu_2} (e^{a y^*} - 1) \ln \left(\frac{F \mu_1 p}{(1 - \mu_2)(e^{a y^*} - \mu_1(1 - p))} \right). \quad (50)$$

When skill parameter a becomes larger than a_C , we observe an abrupt reduction of x_1^* , x_2^* values while the value of y^* grows fast, i.e., qualitatively the same scenario as

shown in Figure 8 in case of map (36). However, considering the dynamical behaviour, there are differences. The Jury criteria may be expressed as

$$J_1(a) = (1 - \mu_2)(1 - a c x_1^*) + (a c x_1^* - e^{-a y^*}) \cdot (B_2 + (\mu_1 p B_3 - \mu_2 B_2)) > 0, \quad (51a)$$

$$J_2(a) = (1 + \mu_2)(1 + a c x_1^*) + (a c x_1^* + e^{-a y^*}) \cdot (B_2 - (\mu_1 p B_3 - \mu_2 B_2)) > 0, \quad (51b)$$

$$J_3(a) = 1 - a c x_1^* |\mu_1 p B_3 - \mu_2 B_2| > 0, \quad (51c)$$

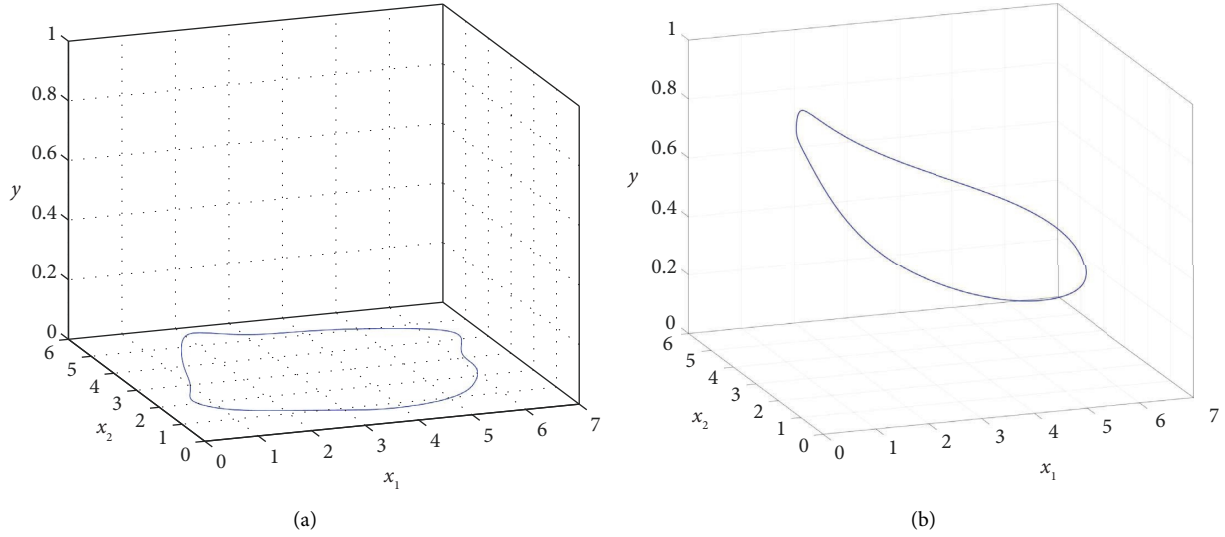


FIGURE 12: Invariant curves generated by map (37). (a) $(\mu_1, \mu_2, p, F, c, a) = (1, 0.1, 0.8, 15, 0.5, 0.7)$. (b) $(\mu_1, \mu_2, p, F, c, a) = (1, 0.5, 0.8, 15, 0.5, 0.61)$.

$$J_4(a) = \left| 1 - (acx_1^*)^2 (\mu_1 p B_3 - \mu_2 B_2)^2 \right| - \left| acx_1^* (B_2 + \mu_2) + (\mu_1 p B_3 - \mu_2 B_2) \cdot (acx_1^* (acx_1^* + \mu_2 + B_2 e^{-ay^*}) - e^{-ay^*}) \right| > 0, \quad (51d)$$

where

$$\begin{aligned} B_2 &= \mu_1 (1 - p) - Fe^{-x^*} x_2^*, \\ B_3 &= Fe^{-x^*} (1 - x_2^*), \end{aligned} \quad (52)$$

from which we obtain the following: given that F is sufficiently small and that the prey possesses a precocious semelparous life history, and there exists an interval $a_C < a < a_m$ where the fixed point is stable, but when $a = a_m$, we find in contrast to previously discussed cases that (x_1^*, x_2^*, y^*) fails to be hyperbolic as $J_2(a_m)$ becomes zero. When $a > a_m$, we find stable period 2-orbits as shown in Figure 13(a) which is followed by chaotic oscillations when a exceeds 7.439, see Figure 13(b). There are no cycles of period 2^k , $k > 1$. Moreover, when the fecundity F is increased, the interval $[a_C, a_m]$ shrinks towards zero, and, as expected, the dynamics is 2-periodic in case of small values of a , and chaotic when a becomes larger.

If the prey population possesses a delayed semelparous life history, the impact of predation is somewhat different. For small values of F , there exists an interval where (x_1^*, x_2^*, y^*) is stable, but nonstationary dynamics is introduced as $J_4(a)$ fails to be positive. Hence, when $a > a_m$ and $|a - a_m|$ are small, there is quasistationary dynamics which turns chaotic when a becomes large. However, if F becomes large, the fixed point undergoes a flip bifurcation at threshold, and the dynamics shows great resemblance to the findings in the precocious semelparous case.

Assuming that the prey exhibits a precocious iteroparous life history, the impact of predation is quite similar to the previous discussed case whenever F is sufficiently small. Here, we also find an interval $a_C < a < a_m$ where (x_1^*, x_2^*, y^*) is stable, and stability is lost as the fixed point undergoes a Neimark-Sacker bifurcation at threshold $a = a_m$ where $J_4(a_m) = 0$. Consequently, quasistationary orbits are the outcome when $a > a_m$, and we have not detected periodic or chaotic dynamics. When F becomes larger, the dynamics changes. There is no skill parameter interval where (x_1^*, x_2^*, y^*) is stable, and when $a > a_C$ and $|a - a_C|$ is small, the dynamics is 2-periodic. Through further enlargement of a , we reach a threshold where the second iterate of map (39) undergoes a Neimark-Sacker bifurcation, which means that the dynamics is restricted to two invariant curves as shown in Figure 14. For higher values of a , the curves disappear, and the dynamics is restricted to one invariant curve only.

Finally, turning to the impact of predation on prey species who possess delayed iteroparous life histories, we find that the interval $a_C < a < a_m$ where the fixed point is stable is larger; here, compared to all other cases, we have discussed. Instability is introduced as $J_4(a_m)$ becomes zero, and in case of $a > a_m$, we have only recorded quasistationary dynamics.

Let us turn to case IV, map (39), where only the mature part of the prey population is exposed to harvest. The treatment will be performed in the same way as we did in the case of map (38). The fixed point may be written as

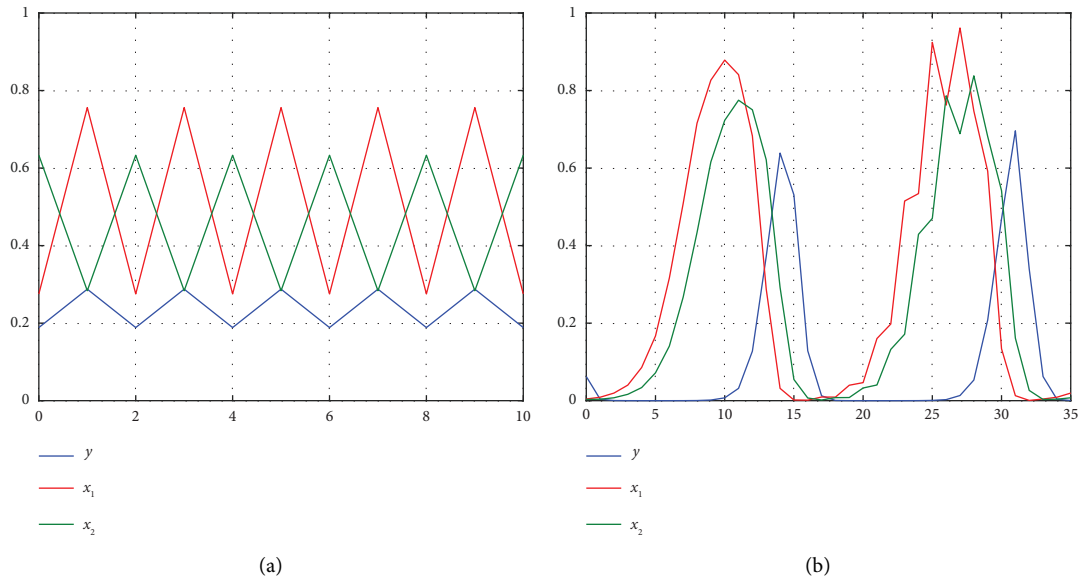


FIGURE 13: (a) Stable 2-cycles. $(\mu_1, \mu_2, p, F, c, a) = (1, 0.1, 0.8, 5, 0.5, 3)$. (b) Chaotic oscillations. Parameter values as in (a), but $a = 10$.

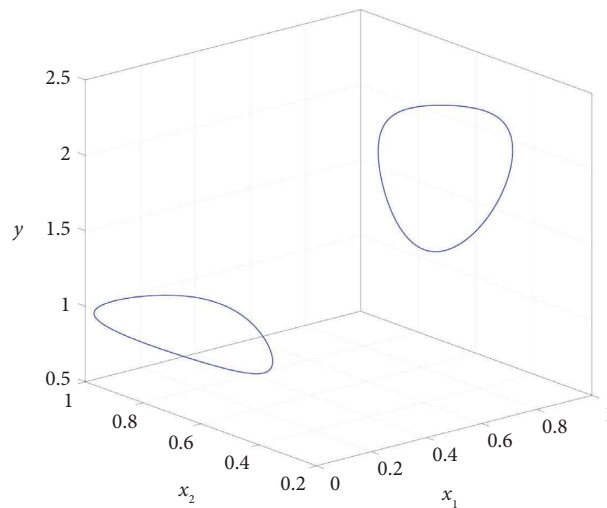


FIGURE 14: Dynamics generated by map (39). Parameter values $(\mu_1, \mu_2, p, F, c, a) = (1, 0.5, 0.8, 15, 0.5, 2)$.

$$(x_1^*, x_2^*, y^*) = \left(\frac{e^{ay^*} - \mu_2}{e^{ay^*} + \mu_1 p - \mu_2} \ln \left(\frac{\mu_1 p F}{(e^{ay^*} - \mu_2)(1 - \mu_1(1 - p))} \right), \frac{\mu_1 p}{e^{ay^*} + \mu_1 p - \mu_2} \ln \left(\frac{\mu_1 p F}{(e^{ay^*} - \mu_2)(1 - \mu_1(1 - p))} \right), y^* \right), \tag{53}$$

and y^* must be found by means of numerical methods from

$$y^* = c(e^{ay^*} - 1) \frac{\mu_1 p}{e^{ay^*} + \mu_1 p - \mu_2} \ln \left(\frac{\mu_1 p F}{(1 - \mu_1(1 - p))(e^{ay^*} - \mu_2)} \right). \tag{54}$$

Stability properties are found in the usual matter by use of the Jury criteria $J_1(a), \dots, J_4(a)$. Assuming that the prey

possesses a precocious semelparous life history, our first finding is that the interval $[a_c, a_m]$ where fixed point (53)

maintains its stability is significantly larger here than in the corresponding Case III. Beyond threshold a_m , the dynamics follows the same pattern as in Case III. There is one more discrepancy. When $a > a_C$ and $|a - a_m|$ is small, an enlargement of the skill parameter results in a larger sub-population x_1^* , confer Case II.

Now, consider prey species who possess delayed semelparous life histories. Assuming that F is small, we find the following differences compared to the precocious semelparous case: (i) the increase of x_1^* when $a > a_C$ and $|a - a_C|$ small is absent, (ii) the skill parameter interval $a_C < a < a_m$ where (x_1^*, x_2^*, y^*) is stable is much larger, (iii) at instability threshold, $J_4(a)$ fails to be positive which means that the fixed point undergoes a Neimark-Sacker bifurcation at threshold. We observe nothing but quasiperiodic orbits when $a > a_m$ except for small parameter windows where the dynamics is periodic (long periods!). However, when F becomes larger, the transfer from stability to instability goes through a flip bifurcation, and there exists a skill parameter interval where the only dynamical outcomes are stable 2-cycles. As the skill parameter is increased, the second iterate of map (39) undergoes a Neimark-Sacker bifurcation, and the dynamics is restricted to two invariant curves which are visited once every second iteration.

Assuming that the prey possesses a precocious iteroparous life history the impact of predation leads to the following results, in case of F small, we find that the interval $[a_C, a_m]$ where the fixed point is stable is smaller than in the corresponding delayed semelparous case but larger than in the precocious semelparous case. (x_1^*, x_2^*, y^*) loses its hyperbolicity when $J_4(a)$ becomes zero and when $a > a_m$, map (39) generates nonstationary dynamics. For larger values of F , the interval $[a_C, a_m]$ shrinks, and instability is introduced when $J_2(a)$ becomes zero. When $a > a_m$, we observe 2-periodic dynamics, and depending on F , chaotic dynamics, see Figures 15(a) and 15(b), or quasistationary dynamics similar to the delayed semelparous case.

Finally, consider the impact of predation on prey species who possess delayed iteroparous life histories. The overall conclusion is that this is where we find the largest skill parameter interval $[a_C, a_m]$ where (x_1^*, x_2^*, y^*) may be stable. Moreover, by the use of the same fecundity values F as we have applied in our previous discussions, $J_4(a) = 0$ at bifurcation threshold $a = a_m$. Beyond a_m , we have only detected invariant curves, and there is no sign of periodical dynamics nor chaotic behaviour.

4. Summary

In this paper, we have analyzed two one-population (prey) models, maps (1) and (2), together with four prey-predator models, maps (36)–(39). The difference between the prey maps (1) and (2) is that in the former, the whole population contributes to density effects, while only the mature sub-population contributes in the latter. As proved, both maps are permanent, and parameter intervals exist where fixed points (3) as well as (40) are stable. The interval where (3) is stable is in general much larger than the other. Hence, a natural conclusion to draw is that whenever $x = x_1 + x_2$

contributes to density effects, and stability properties are better compared to the case where only x_2 contributes. Considering life histories, we find from both models that species who possess a delayed semelparous or iteroparous life history appear to be more stable than species who possess precocious semelparous or iteroparous life histories. Thus, our results both confirm and extend the findings obtained in [13]. Moreover, both maps (1) and (2) undergo supercritical bifurcations at their respective instability thresholds. However, while (1) undergoes a flip bifurcation, map (2) undergoes a Neimark-Sacker bifurcation which has crucial impacts on the nonstationary dynamics. Regarding map (1), there are 2-cycles beyond threshold and, depending on life history, chaotic dynamics as well. We have also detected parameter regions where multiple attractors exist which may possess large trapping regions. Considering map (2), we find in the precocious semelparous case both quasistationary orbits restricted to invariant curves, dynamics with great resemblance of 4-cycles as well as chaotic dynamics. Whenever the population possesses other life histories, nonperiodic orbits and periodic orbits of long period are the only dynamical outcomes.

Let us now turn to the impact of predation. Assuming that F is so small that fixed points (3) and (40) are stable in absence of predators, we find that there exists a skill parameter interval $[a_C, a_m]$ where the various fixed points (x_1^*, x_2^*, y^*) are stable. The smallest interval occurs when the prey possesses a precocious semelparous life history, where only the mature part of the populations x_2 contributes to density effects and the immature part x_1 is the target of predation. On the other hand, we find the largest interval when the life history is of the delayed iteroparous kind, $x = x_1 + x_2$ is responsible for density effects, and x_2 only is exposed to predation. In many respects, the findings above reflect the results from the analyses of maps (1) and (2). Larger values of F imply that the lengths of $[a_C, a_m]$ shrink. When F exceeds a certain threshold, depending on life history, (x_1^*, x_2^*, y^*) will never be stable. A final comment regarding fixed points is that whenever the prey possesses a precocious semelparous life history, and x_2 only is exposed to predation, and a small increase of parameter a actually lead to a larger immature equilibrium population x_1^* . In all other cases, the sizes of x_1^*, x_2^* are reduced when a is increased.

When $a > a_C$ and $|a - a_C|$ are small, an increase of a acts in a stabilizing way. However, when a approaches a_m , it becomes destabilizing, and at threshold a_m , the various fixed points (x_1^*, x_2^*, y^*) lose their hyperbolicity. In most cases, this occurs when $J_4(a_m) = 0$, i.e., through a Neimark-Sacker bifurcation. Therefore, beyond instability threshold, we find quasiperiodic orbits, and depending on life histories, maps (36)–(39) may generate periodic dynamics of long period as well as chaotic dynamics through further increase of a . Chaotic dynamics appears to be rare events in the delayed cases. In contrast to the findings above, if the prey possesses a precocious semelparous life history, the whole population is responsible for density effects, and x_1 only is exposed to predation, and $J_2(a_m)$ becomes zero prior to $J_4(a_m)$. Thus, the dynamics beyond threshold is 2-periodic or chaotic if the

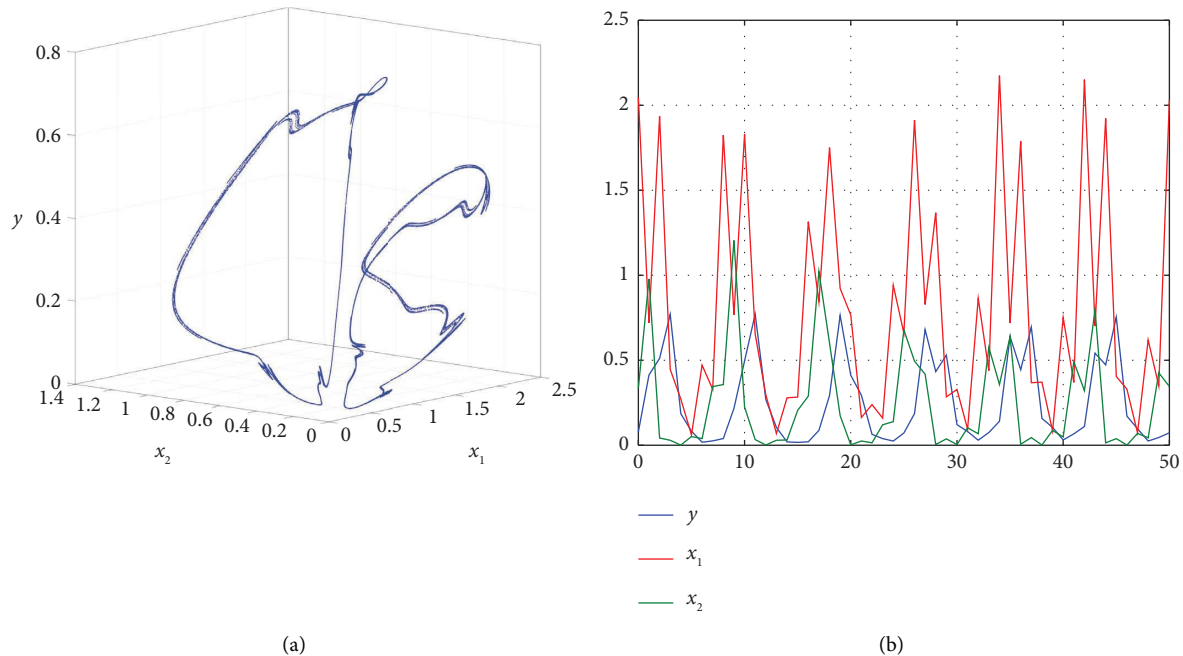


FIGURE 15: (a) Chaotic dynamics generated by map (39). Parameter values $(\mu_1, \mu_2, p, F, c, a) = (1, 0.5, 0.8, 10, 0.5, 7.79)$. (b) The corresponding time series.

skill parameter becomes sufficiently large (perhaps somewhat unexpected, we do not observe periodic orbits of period 2^k , $k > 1$). We have also detected the dynamics reported above when F is large in the delayed semelparous case.

Data Availability

No data were used to support this study.

Conflicts of Interest

The authors declare that they have no conflicts of interest.

Acknowledgments

The publication charges for this article have been funded by a grant from the publication fund of UiT The Arctic University of Norway.

References

- [1] J. Guckenheimer, G. Oster, and A. Ipaktchi, "The dynamics of density dependent population models," *Journal of Mathematical Biology*, vol. 4, no. 2, pp. 101–147, 1977.
- [2] L. Pennycuik, "A computer model of the Oxford great tit population," *Journal of Theoretical Biology*, vol. 22, no. 3, pp. 381–400, 1969.
- [3] S. A. Levin and C. P. Goodyear, "Analysis of an age-structured fishery model," *Journal of Mathematical Biology*, vol. 9, no. 3, pp. 245–274, 1980.
- [4] J. A. L. Silva and T. G. Hallam, "Effects of delay, truncations and density dependence in reproduction schedules on stability of nonlinear Leslie matrix models," *Journal of Mathematical Biology*, vol. 31, no. 4, pp. 367–395, 1993.
- [5] E. Mj-lhus and A. Wikan, "Overcompensatory recruitment and generation delay in discrete age-structured population models," *Journal of Mathematical Biology*, vol. 35, no. 2, pp. 195–239, 1996.
- [6] N. V. Davydova, O. Diekmann, and S. van Gils, "Year class coexistence or competitive exclusion for strict biennials," *Journal of Mathematical Biology*, vol. 46, no. 2, pp. 95–131, 2003.
- [7] J. M. Cushing, "Nonlinear semelparous Leslie models," *Mathematical Biosciences and Engineering*, vol. 3, no. 1, pp. 17–36, 2006.
- [8] J. M. Cushing and S. M. Henson, "Stable bifurcations in semelparous Leslie models," *Journal of Biological Dynamics*, vol. 6, no. sup2, pp. 80–102, 2012.
- [9] J. M. Cushing, "On the fundamental bifurcation theorem for semelparous Leslie models," in *Dynamics, Games and Science*, J. P. Bourguignon, R. Jeltsch, A. A. Pinto, and M. Viana, Eds., Springer International Publishing, Berlin, Germany, 2015.
- [10] A. Wikan, "An analysis of a semelparous population model with density-dependent fecundity and density-dependent survival probabilities," *Journal of Applied Mathematics*, vol. 2017, Article ID 8934295, 14 pages, 2017.
- [11] H. Behncke, "Periodical cicadas," *Journal of Mathematical Biology*, vol. 40, no. 5, pp. 413–431, 2000.
- [12] O. Diekmann and R. Planqué, "The winner takes it all: how semelparous insects can become periodical," *Journal of Mathematical Biology*, vol. 80, no. 1-2, pp. 283–301, 2020.
- [13] M. G. Neubert and H. Caswell, "Density-dependent vital rates and their population dynamic consequences," *Journal of Mathematical Biology*, vol. 41, no. 2, pp. 103–121, 2000.
- [14] R. Kon, Y. Saito, and Y. Takeuchi, "Permanence of single species stage-structured models," *Journal of Mathematical Biology*, vol. 48, no. 5, pp. 515–528, 2004.
- [15] W. Govaerts and R. K. Ghaziani, "Numerical bifurcation analysis of a nonlinear stage structured cannibalism

- population model,” *Journal of Difference Equations and Applications*, vol. 12, no. 10, pp. 1069–1085, 2006.
- [16] R. F. Costantino, R. A. Desharnais, J. M. Cushing, and B. Dennis, “Chaotic dynamics in an insect population,” *Science*, vol. 275, no. 5298, pp. 389–391, 1997.
- [17] M. G. Neubert and M. Kot, “The subcritical collapse of predator populations in discrete-time predator-prey models,” *Mathematical Biosciences*, vol. 110, no. 1, pp. 45–66, 1992.
- [18] A. Wikan, “From chaos to chaos. An analysis of a discrete age-structured prey-predator model,” *Journal of Mathematical Biology*, vol. 43, no. 6, pp. 471–500, 2001.
- [19] H. N. Agiza, E. M. Elabbasy, H. El-Metwally, and A. A. Elsadany, “Chaotic dynamics of a discrete prey predator model with Holling type II,” *Nonlinear Analysis: Real World Applications*, vol. 10, no. 1, pp. 116–129, 2009.
- [20] Z. Eskandari, J. Alidousti, Z. Avazzadeh, and J. A. Tenreiro Machado, “Dynamics and bifurcations of a discrete-time prey-predator model with Allee effect on the prey population,” *Ecological Complexity*, vol. 48, Article ID 100962, 2021.
- [21] S. M. S. Rana and U. Kulsum, “Bifurcation analysis and chaos control in a discrete-time predator-prey system of Leslie type with simplified Holling type IV functional response,” *Discrete Dynamics in Nature and Society*, vol. 2017, Article ID 9705985, 11 pages, 2017.
- [22] U. Saeed, I. Ali, and Q. Din, “Neimark-Sacker bifurcation and chaos control in discrete-time predator-prey model with parasites,” *Nonlinear Dynamics*, vol. 94, no. 4, pp. 2527–2536, 2018.
- [23] Q. Din, “Stability, bifurcation analysis and chaos control for a predator-prey system,” *Journal of Vibration and Control*, vol. 25, no. 3, pp. 612–626, 2019.
- [24] A. Q. Khan and T. Khaliq, “Neimark-Sacker bifurcation and hybrid control in a discrete-time Lotka-Volterra model,” *Mathematical Methods in the Applied Sciences*, vol. 43, no. 9, pp. 5887–5904, 2020.
- [25] A. Wikan, “On the interplay between cannibalism and harvest in stage-structured population models,” *Journal of Marine Biology*, vol. 2015, Article ID 580520, 8 pages, 2015.
- [26] J. Guckenheimer and P. Holmes, “Nonlinear oscillations, dynamical systems, and bifurcations of vector fields,” *Applied Mathematical Sciences*, Springer-Verlag, Berlin, Germany, 1990.
- [27] A. Wikan, “An analysis of discrete stage-structured prey and prey-predator population models,” *Discrete Dynamics in Nature and Society*, vol. 201711 pages, Article ID 9475854, 2017.
- [28] A. Hastings, “Age-dependent predation is not a simple process. II. Wolves, ungulates, and a discrete time model for predation on juveniles with a stabilizing tail,” *Theoretical Population Biology*, vol. 26, no. 2, pp. 271–282, 1984.